Conversion Loss and Noise of Microwave and Millimeter-Wave Mixers: Part 1—Theory

DANIEL N. HELD, MEMBER, IEEE, AND ANTHONY R. KERR, ASSOCIATE MEMBER, IEEE

Abstract—**An analysis is presented for the conversion loss and noise of microwave and millimeter-wave mixers. The analysis includes the effects of nonlinear capacitance, arbitrary embedding impedances, nonideality of microwave diodes, and shot, thermal, and scattering noise generated in the diode. Correlation of down-converted components of the time-varying shot noise is shown to explain the "anomalous" noise observed in millimeter-wave mixers. Part 1 of the paper presents the theoretical basis for predicting mixer performance, while Part 2 compares theoretical and experimental results for mixers operating at 87 and 115 GHz.**

I. Introduction

THE BASIC principles of frequency conversion using crystal diodes were first studied in depth by Torrey and Whitmer [1] in 1948. Since then attempts at a more accurate analysis of microwave mixer performance have been limited by the complexity of the nonlinear problem and by a lack of understanding of the noise properties of pumped diodes. Practical developments in the design of mixers and mixer diodes have resulted in a number of commonly used designs whose conversion loss and noise figure are often within a few decibels of the theoretical best values predicted for idealized switching mixers. This paper and its companion paper (Part 2) attempt to close the gap between theory and practice.

Following Torrey and Whitmer's original work, the assumption of a sinusoidal local oscillator (LO) voltage across an exponential resistive diode was often used, with its implicit assumption that the diode was short-circuited at all harmonics of the LO. The effects of the parasitic series resistance and capacitance (assumed constant) of the mixer diode were investigated using approximate methods by Sharpless [2], Messenger and McCoy [3], Mania and Stracca [4], and Kerr [5]; and a new and intuitive approach to mixer analysis was taken by Barber [6], who approximated the diode by a switch whose pulse-duty ratio determined the conversion properties of the mixer. However, all these approaches required simplifying assumptions about the termination of higher order sidebands and ignored the effects of the nonlinear diode capacitance. Agreement between theory and experiment was at best within a few decibels in conversion loss and noise figure.

An important work by Saleh [7] in 1971 studied the effects of local oscillator waveforms and higher order sideband terminations on resistive mixers, and demonstrated that these characteristics must be considered if an accurate analysis is to be made. The problem of a more exact analysis of a microwave mixer has been tackled recently by Egami [8], who performed a numerical nonlinear analysis for a known diode and embedding impedance, followed by a small-signal conversion loss analysis. Egami assumed a constant junction capacitance and used a harmonic balance technique to solve the nonlinear problem, considering three harmonics of the local oscillator.

In recent years considerable misunderstanding has arisen on the subject of mixer noise. The correlation properties of shot noise in vacuum tube mixers were understood by Strutt [9] in 1946 and since then van der Ziel and Waters [10], [11], Kim [12], and Dragone [13] have further developed this theory. The misunderstanding seems to have arisen with the assumption, by Messenger and McCoy [3], that a mixer and a passive attenuator have similar noise properties and that the temperature of this equivalent attenuator is "the time average of the static noise characteristic" of the diode. This led to a widely held belief that for a Schottky diode mixer, the noise-temperature ratio [3] $t \simeq 1$, and to the subsequent observation of an "anomalous" component of noise in millimeter-wave mixers [14].

In the present paper the large-signal nonlinear problem and the small-signal linear problem are presented in forms suitable for computer solution. Arbitrary embedding impedances are allowed at the harmonics of the LO and at all the sideband frequencies, and any diode capacitance law can be assumed. The shot-noise theories of Strutt [9], van der Ziel [11], Kim [12], and Dragone [13] are extended to include the effects of arbitrary sideband terminations, as well as thermal (Johnson) noise and scattering noise, resulting in a noise correlation matrix which is compatible with the formulation of the small-signal mixer analysis. The microwave properties of small Schottky-barrier diodes are discussed, and it is shown that skin effect, thermal time constants, and depletion layer fringing effects can all be significant in determining the mixing properties of the diode.

The theory presented in this paper is experimentally verified in a companion paper (Part 2) in which theoretical loss and noise predictions for millimeter-wave mixers are shown to be in good agreement with experiment.

II. Nonlinear Analysis

The small-signal loss and noise properties of a mixer are governed by the large-signal current and voltage waveforms

Manuscript received February 18, 1977; revised May 12, 1977.

D. N. Held was with the Department of Electrical Engineering, Columbia University, New York, NY 10027. He is now with the Jet Propulsion Laboratory, California Institute of Technology, Pasadena, CA 91103.

A. R. Kerr is with the NASA Institute for Space Studies, Goddard Space Flight Center, New York, NY 10025.

0018-9480/78/0200-0049$00.75

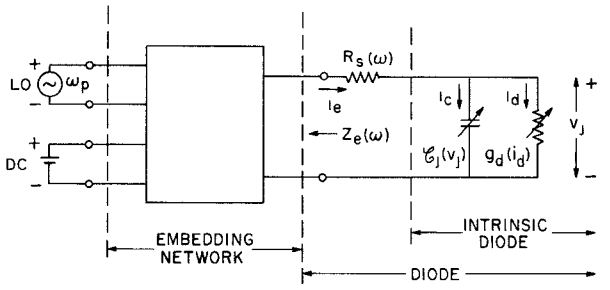

Fig. 1. Equivalent circuit of the mixer. The intrinsic diode $\mathscr{C}_j$ and g_d is nonlinear and is characterized in the time domain, while the diode series resistance R_s and the embedding impedance Z_e are linear and are best represented in the frequency domain.

produced at the diode by the LO. The steady-state large-signal response of the mixer circuit of Fig. 1 can be described in terms of the Fourier coefficients of the voltage and current v_j and i_e. Thus

$$v_j(t) = \sum_{k=-\infty}^{\infty} V_k e^{jk\omega_p t}, \qquad V_k = V^*_{-k} \tag{1}$$

$$i_e(t) = i_c(t) + i_d(t) = \sum_{k=-\infty}^{\infty} I_{e_k} e^{jk\omega_p t}, \qquad I_{e_k} = I^*_{e_{-k}} \tag{2}$$

where ω_p is the LO frequency. Two sets of boundary conditions must be satisfied simultaneously by these quantities. The first, imposed by the diode, is most easily expressed in the time domain, while the second set, imposed by the embedding network, is for our purposes more conveniently considered in the frequency domain. At the diode

$$i_d = i_0[\exp(\alpha v_j) - 1] \tag{3}$$

and

$$i_c = \mathscr{C}_j \frac{dv_j}{dt} \tag{4}$$

where

$$\mathscr{C}_j = \mathscr{C}_{j_0}\left(1 - \frac{v_j}{\phi}\right)^{-\gamma} \tag{5}$$

and

$$\alpha = q/\eta kT. \tag{6}$$

From (3) the incremental conductance of the diode

$$g_d = \frac{di_d}{dv_j} = \alpha(i_d + i_0) \simeq \alpha i_d. \tag{7}$$

The embedding network requires that

$$V_k = -I_{e_k}[Z_e(k\omega_p) + R_s(k\omega_p)], \qquad k = \pm 2, \pm 3, \cdots, \pm\infty \tag{8a}$$

$$V_{\pm 1} = V_p - I_{e_{\pm 1}}[Z_e(\pm\omega_p) + R_s(\pm\omega_p)] \tag{8b}$$

$$V_0 = V_{\mathrm{dc}} - I_{e_0}[Z_e(0) + R_s(0)] \tag{8c}$$

where V_p and V_{dc} are the LO and dc-bias voltages, respectively. The frequency dependence of R_s is due to skin effect and is discussed in Section V.

Methods for solving the nonlinear mixer problem have been described by several authors [15]–[17]. However, only that of Gwarek [17] appears capable of handling the case in which the diode capacitance is a function of junction voltage and in which a large number (six or seven) of harmonics of the LO are considered. Using an IBM 360/95 computer, we have found that with Gwarek's method convergence is achieved in about two seconds. The degree of convergence of the solution is determined using the convergence parameter described by Kerr [16]. It is assumed that there is one unique steady-state solution; the possibility of multiple solutions, mentioned in [16] is beyond the scope of this work.

Having determined the LO waveforms at the diode, (3)–(7) give $i_d(t)$, $g_d(t)$, and $\mathscr{C}_j(t)$. These may be expressed as Fourier series:

$$i_d(t) = \sum_{k=-\infty}^{\infty} I_k \exp(jk\omega_p t), \qquad I_k = I^*_{-k} \tag{9}$$

$$g_d(t) = \sum_{k=-\infty}^{\infty} G_k \exp(jk\omega_p t), \qquad G_k = G^*_{-k} \tag{10}$$

and

$$\mathscr{C}_j(t) = \sum_{k=-\infty}^{\infty} C_k \exp(jk\omega_p t), \qquad C_k = C^*_{-k}. \tag{11}$$

These quantities, together with the embedding impedance $Z_e(\omega)$, determine the small-signal properties of the mixer.

III. Small-Signal Analysis

Knowing the Fourier coefficients of the diode capacitance and conductance, it is possible to construct the small-signal conversion matrix for the diode [1], [17]. This matrix interrelates the various sideband frequency components of the small-signal current and voltage δI_m and δV_m shown in Fig. 2. The subscript notation for the sideband quantities follows that of Saleh [7]; subscript m indicates frequency $\omega_0 + m\omega_p$, where ω_p and ω_0 are the LO and intermediate frequencies. Thus $Z_{e_m} = Z_e(\omega_m) = Z_e(\omega_0 + m\omega_p)$. The conversion matrix $\boldsymbol{Y}$ is a square matrix defined by

$$\boldsymbol{\delta I} = \boldsymbol{Y}\boldsymbol{\delta V}$$

where

$$\boldsymbol{\delta I} = [\cdots, \delta I_1, \delta I_0, \delta I_{-1}, \cdots]^T$$

and

$$\boldsymbol{\delta V} = [\cdots, \delta V_1, \delta V_0, \delta V_{-1}, \cdots]^T. \tag{12}$$

For convenience, the row and column numbering of all matrices and vectors in this paper will correspond with the sideband numbering. For example,

$$\boldsymbol{Y} \equiv \begin{array}{c} \text{row } \# \\ \vdots \\ 1 \\ 0 \\ -1 \\ \vdots \end{array} \begin{bmatrix} & \vdots & \vdots & \vdots & \\ \cdots & Y_{11} & Y_{10} & Y_{1-1} & \cdots \\ \cdots & Y_{01} & Y_{00} & Y_{0-1} & \cdots \\ \cdots & Y_{-11} & Y_{-10} & Y_{-1-1} & \cdots \\ & \vdots & \vdots & \vdots & \end{bmatrix}.$$

$$\cdots \quad 1 \quad 0 \quad -1 \quad \cdots$$

column #

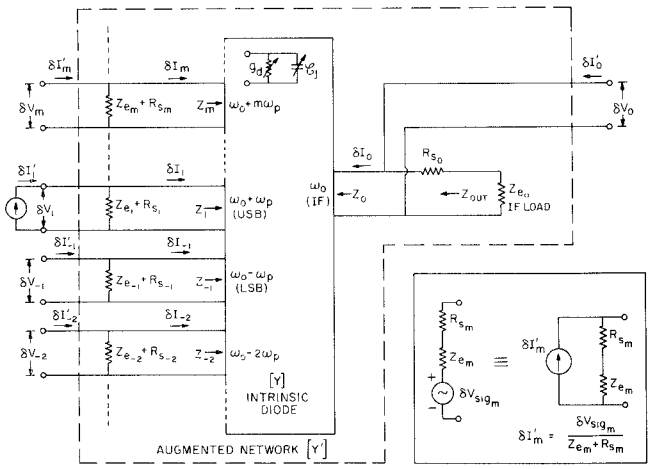

Fig. 2. Small-signal representation of the mixer as a multifrequency linear multiport network. The voltage and current δV_m and δI_m at any port m are the small-signal components at frequency $(\omega_0 + m\omega_p)$ appearing at the intrinsic diode; each port represents one sideband frequency. The conversion matrix $\boldsymbol{Y}$ is the admittance matrix of the intrinsic diode. The augmented network (broken line) includes all the sideband embedding impedances Z_{e_m} and is characterized by the augmented admittance matrix $\boldsymbol{Y}'$. During normal mixer operation the equivalent signal current generator $\delta I'$ is connected at port 1 of the augmented network, the other ports being open-circuited. In the noise analysis, equivalent noise current sources $\delta I'_{S_m}$ and $\delta I'_{T_m}$ are connected to all ports. The inset shows the relation between the signal source δV_{sig_m} at the mth sideband and its equivalent current source $\delta I'_m$.

Using this notation the elements of $\boldsymbol{Y}$ are given by [1], [17]

$$Y_{mn} = G_{m-n} + j(\omega_0 + m\omega_p)C_{m-n} \tag{13}$$

where G_k and C_k are the Fourier coefficients of the diode conductance and capacitance as defined in (10) and (11).

It is convenient to form an augmented Y matrix, $\boldsymbol{Y}'$, which is the admittance matrix of the multiport network outlined by the broken line in Fig. 2. This augmented network contains the whole mixer, including all its external terminating impedances Z_{e_m}, but does not contain signal sources associated with these terminations. Signal sources are replaced by equivalent current sources $\delta I'_m$ connected across $(Z_{e_m} + R_{s_m})$ as shown in Fig. 2 (inset). The ports of the augmented network are all normally open-circuited. For the augmented network

$$\boldsymbol{\delta I' = Y' \delta V} \tag{14}$$

where the elements of $\boldsymbol{\delta I'}$ are defined in Fig. 2, and

$$\boldsymbol{Y' = Y + \text{diag}}\left[\frac{1}{Z_{e_m} + R_{s_m}}\right]. \tag{15}$$

Inverting (14) gives

$$\boldsymbol{\delta V = Z' \delta I'} \tag{16}$$

where

$$\boldsymbol{Z' = (Y')^{-1}}. \tag{17}$$

A. Mixer Port Impedances

To determine the port impedance Z_m, defined in Fig. 2, the corresponding embedding impedance Z_{e_m} is open-circuited, enabling Z_m to be measured at port m of the augmented network. It follows that

$$Z_m = Z'_{mm,\infty} \tag{18}$$

where the subscript ∞ indicates that Z'_{mm} (the mmth element of $\boldsymbol{Z'}$) is evaluated with $Z_{e_m} = \infty$. In particular the IF output impedance is (see Fig. 2)

$$Z_{\text{out}} = Z_0 + R_{s_0} = Z'_{00,\infty} + R_{s_0}. \tag{18a}$$

For a microwave mixer the embedding impedance at all frequencies other than the IF is defined by the mixer geometry. However, the IF load impedance Z_{e_0} can usually be adjusted for optimum performance using a matching circuit. *Throughout the rest of this paper it will be assumed that the IF port is conjugate-matched,*[1] and IF-matched $\boldsymbol{Y'}$ and $\boldsymbol{Z'}$ matrices will be implied.

B. Conversion Loss

The conversion loss of a mixer

$$L = \frac{\text{Power available from source } Z_{e_1}}{\text{Power delivered to load } Z_{e_0}}. \tag{19}$$

For the purposes of analysis L may be expressed as the product of three separate loss components:

$$L = K_0 L' K_1 \tag{20}$$

where

$$K_0 = \frac{\text{Power delivered to } (Z_{e_0} + R_{s_0})}{\text{Power delivered to } Z_{e_0}} = \frac{\text{Re}\,[Z_{e_0} + R_{s_0}]}{\text{Re}\,[Z_{e_0}]} \tag{21}$$

$$L' = \frac{\text{Power available from } (Z_{e_1} + R_{s_1})}{\text{Power delivered to } (Z_{e_0} + R_{s_0})} \tag{22}$$

and

$$K_1 = \frac{\text{Power available from } Z_{e_1}}{\text{Power available from } (Z_{e_1} + R_{s_1})} = \frac{\text{Re}\,[Z_{e_1} + R_{s_1}]}{\text{Re}\,[Z_{e_1}]}. \tag{23}$$

K_0 and K_1 account for loss in the series resistance at the IF and signal frequencies, while L' is the conversion loss of the intrinsic mixer with no series resistance. Using (22) and (16),

$$L' = \frac{1}{\text{Re}\,[\delta V_0 \delta I_0^*]} \frac{|\delta I'_1|^2 |Z_{e_1} + R_{s_1}|^2}{4\,\text{Re}\,[Z_{e_1} + R_{s_1}]} = \frac{1}{4|Z'_{01}|^2} \frac{|Z_{e_0} + R_{s_0}|^2}{\text{Re}\,[Z_{e_0} + R_{s_0}]} \frac{|Z_{e_1} + R_{s_1}|^2}{\text{Re}\,[Z_{e_1} + R_{s_1}]}. \tag{24}$$

From (20), (21), (23), and (24), the conversion loss

$$L = \frac{1}{4|Z'_{01}|^2} \frac{|Z_{e_0} + R_{s_0}|^2}{\text{Re}\,[Z_{e_0}]} \frac{|Z_{e_1} + R_{s_1}|^2}{\text{Re}\,[Z_{e_1}]}. \tag{25}$$

[1] Note that although a conjugate-match at the IF port results in maximum power transfer, the signal port should not in general be conjugate-matched for minimum conversion loss [7].

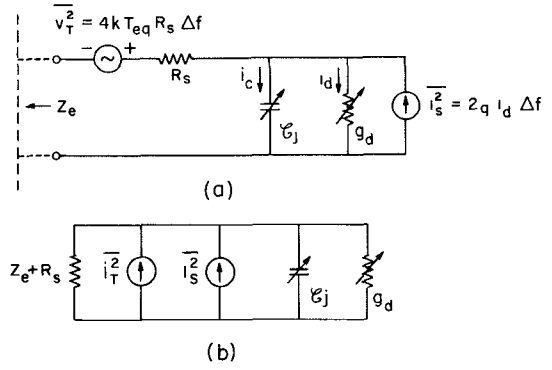

Fig. 3. (a) Noise equivalent circuit of the mixer. (b) The equivalent circuit with the thermal noise source $\overline{v_T^2}$ transformed to a current source $\overline{i_T^2}$ given by equation (27). The sideband components of the noise sources $\overline{i_T^2}$ and $\overline{i_S^2}$ can then be treated in the same way as the equivalent external small-signal currents $\delta I'_m$ in Fig. 2.

Equation (25) may be generalized to give the conversion loss from any sideband j to any other sideband i.

$$L_{ij} = \frac{1}{4|Z'_{ij}|^2} \frac{|Z_{e_i} + R_{s_i}|^2}{\mathrm{Re}\,[Z_{e_i}]} \frac{|Z_{e_j} + R_{s_j}|^2}{\mathrm{Re}\,[Z_{e_j}]}. \tag{26}$$

IV. Mixer Noise

The sources of noise in a Schottky diode are 1) thermal noise in the series resistance, 2) shot noise generated by current flow across the barrier, and 3) noise due to phonon scattering and, in gallium arsenide, intervalley scattering [22]. In room-temperature mixers shot and thermal noise predominate, with scattering noise contributing typically only 5–10 percent to the overall mixer noise, as is shown in Part 2 of this paper. We have not attempted an exact analysis of scattering noise but assume that it can be approximated by an increase in the noise temperature of the series resistance.

The equivalent circuit of the diode including noise sources is shown connected to the embedding network in Fig. 3(a). Fig. 3(b) shows the same circuit transformed to a configuration more compatible with the mixer equivalent circuit of Fig. 2; the thermal noise source $\overline{v_T^2}$ has been replaced by an equivalent current source $\overline{i_T^2}$. As seen by the intrinsic diode (g_d and $\mathscr{C}_j$),

$$\overline{i_T^2} = \frac{4kT_{eq}R_s\Delta f}{|Z_e + R_s|^2} \tag{27a}$$

but, as seen by the IF load impedance Z_{e_0},

$$\overline{i_T^2} = \frac{4kT_{eq}R_s\Delta f}{|Z_0|^2} \tag{27b}$$

where Z_0 is the output impedance of the intrinsic diode as defined in Fig. 2. The shot-noise current source

$$\overline{i_S^2} = 2qi_d\Delta f. \tag{28}$$

A. Shot Noise

The diode shot noise given by (28) is a function of the instantaneous flow of current i_d across the barrier, produced by the LO. Since $i_d(t)$ is periodic, the shot-noise current can be regarded as a stationary white noise current modulated at the LO frequency ω_p. The properties of this modulated shot noise have been studied by Strutt [9], Kim [12], van der Ziel [11], and Dragone [13], and the present analysis is based on their work.

First, we shall consider the *unmodulated* shot-noise current to be composed of pseudosinusoidal currents [18], [19] $\delta\mathscr{I}_{S_m} \exp[j(\omega_0 + m\omega_p)t + j\phi_m]$ at each of the sideband frequencies $\omega_m = \omega_0 + m\omega_p$, $m = 0, \pm 1, \cdots, \pm\infty$. All other frequency components of the noise can be disregarded since they cannot contribute to the IF output of the mixer. Next, consider each of the currents $\delta\mathscr{I}_{S_m}$ to be modulated by the local oscillator (ω_p), generating modulation products at all the frequencies $\omega_m + n\omega_p$, $n = 0, \pm 1, \pm 2, \cdots, \pm\infty$, which are the sideband frequencies ω_{m+n}. The modulation products are present at the terminals of the intrinsic diode and will be converted to the output frequency as described by (16). Clearly their individual outputs will be correlated. The random phase variable ϕ_m is preserved in these output components but is eliminated when we finally consider a finite bandwidth and take the ensemble average of a set of pseudosinusoidal currents in a narrow band about each of the frequencies ω_m.

Let $\delta I'_{S_m}$ denote the complex amplitude of the pseudosinusoidal noise current at sideband frequency ω_m. $\delta I'_{S_m}$ contains components due to the modulation products of all the currents $\delta\mathscr{I}_S$ and is therefore the shot-noise input current at port m of the mixer, which corresponds to a signal input current $\delta I'_m$ in Fig. 2. The vector $\boldsymbol{\delta I'_S}$ is defined as $[\cdots, \delta I'_{S_1}, \delta I'_{S_0}, \delta I'_{S_{-1}}, \cdots]^T$. Equation (16) now enables the IF output noise voltage due to shot noise to be determined:

$$\delta V_{S_0} = \boldsymbol{Z'_0}\,\boldsymbol{\delta I'_S} \tag{29}$$

where $\boldsymbol{Z'_0}$ is the zeroth row of the square matrix $\boldsymbol{Z'}$. Taking the ensemble average[2] of $|\delta V_{S_0}|^2$ (which corresponds considering a nonzero bandwidth),

$$\langle |\delta V_{S_0}|^2 \rangle = \boldsymbol{Z'_0}\langle \boldsymbol{\delta I'_S}\,\boldsymbol{\delta I'^{\dagger}_S} \rangle \boldsymbol{Z'^{\dagger}_0}. \tag{30}$$

The square matrix $\langle \boldsymbol{\delta I'_S}\,\boldsymbol{\delta I'^{\dagger}_S} \rangle$ is known as the *correlation matrix* for the mixer, since the (m,n) element describes the correlation between the components of shot noise at sideband frequencies ω_m and ω_n. Dragone [13] has evaluated this matrix, obtaining

$$\langle \delta I'_{S_m}\,\delta I'^{*}_{S_n} \rangle = 2qI_{m-n}\Delta f \tag{31}$$

where I_{m-n} is one of the Fourier coefficients of the local oscillator current $i_d(t)$ as defined in (9).

A different approach leading to the same result has been taken by van der Ziel [11] in his analysis of shot noise in mixers. The shot noise, caused by electrons crossing the depletion layer of the diode, is considered as a series of impulsive deviations from the noiseless diode current. The

[2] The symbol $\langle \cdots \rangle$ denotes statistical (or ensemble) average as opposed to time average which is denoted by an overbar. Superscripts T and $\dagger$ denote, respectively, the transpose and the complex conjugate transpose of a matrix or vector.

spectrum of each current impulse is flat and the phase is linear with frequency, its slope depending on the time of occurrence of the impulse. The different frequency components ω_m are down-converted according to (16) and have phases related to the time of occurrence of the impulse and to the LO phase. Summing the separate effects of all such impulses gives the output voltage due to shot noise, including the effects of correlation between the components. Van der Ziel gives the example of a simple two-port mixer as an illustration of the effect of shot-noise correlation.

B. Thermal Noise

It was shown above ((27) and Fig. 3) that the thermal noise generated in the series resistance of the diode can be regarded as a noise current source $\overline{i_T^2}$ across the terminals of the intrinsic diode.

Since R_s is assumed to be time-invariant, down-converted thermal noise will have no correlated components; quasisinusoidal components $\delta I'_{T_m}$ at the sideband frequencies ω_m give rise to an output voltage (using (16))

$$\delta V_{T_0} = \boldsymbol{Z}'_0 \boldsymbol{\delta I}'_T \tag{32}$$

where $\boldsymbol{\delta I}'_T = [\cdots, \delta I'_{T_1}, \delta I'_{T_0}, \delta I'_{T_{-1}}, \cdots]^T$, and $\boldsymbol{Z}'_0$ is a row of the matrix $\boldsymbol{Z}'$.

Taking the ensemble average of $|\delta V_{T_0}|^2$ gives

$$\langle \delta V_{T_0}^2 \rangle = \boldsymbol{Z}'_0 \langle \boldsymbol{\delta I}'_T \, \boldsymbol{\delta I}'^{\dagger}_T \rangle \boldsymbol{Z}'^{\dagger}_0. \tag{33}$$

The square matrix $\langle \boldsymbol{\delta I}'_T \, \boldsymbol{\delta I}'^{\dagger}_T \rangle$ is again the correlation matrix (cf. (30)), but since $\delta I'_{T_m}$ and $\delta I'_{T_n}$ are uncorrelated for $m \neq n$, it is a diagonal matrix with the elements

$$\langle \delta I'_{T_m} \, \delta I'^{*}_{T_m} \rangle = \frac{4kT_{eq}R_{s_m}\Delta f}{|Z_{e_m} + R_{s_m}|^2}, \qquad m \neq 0 \tag{34a}$$

$$= \frac{4kT_{eq}R_{s_0}\Delta f}{|Z_0|^2}, \qquad m = 0. \tag{34b}$$

C. Total Mixer Noise

Combining the shot and thermal noise output voltages given by (30) and (33) gives the total noise output voltage appearing across the series combination of the IF load and the diode series resistance (see Fig. 2):

$$\langle \delta V_{N_0}^2 \rangle = \boldsymbol{Z}'_0 \{ \langle \boldsymbol{\delta I}'_S \, \boldsymbol{\delta I}'^{\dagger}_S \rangle + \langle \boldsymbol{\delta I}'_T \, \boldsymbol{\delta I}'^{\dagger}_T \rangle \} \boldsymbol{Z}'^{\dagger}_0 \tag{35}$$

where the shot and thermal noise correlation matrices $\langle \boldsymbol{\delta I}'_S \, \boldsymbol{\delta I}'^{\dagger}_S \rangle$ and $\langle \boldsymbol{\delta I}'_T \, \boldsymbol{\delta I}'^{\dagger}_T \rangle$ are given by (31) and (34). It is assumed here that the effects of scattering noise are fairly small and are equivalent to a small increase in the value of the equivalent noise temperature of the diode series resistance T_{eq} in (27) and (34). The magnitude of this increase can be estimated from the current waveform of the pumped diode and from measurements on the dc biased diode, as described in Part 2 of this paper.

The equivalent input noise temperature T_M of a two-frequency mixer (no external image termination) may be defined in terms of a noiseless but otherwise identical mixer: T_M is the temperature to which the source conductance of the noiseless mixer must be heated in order to deliver to the IF load the same noise power as the noisy mixer delivers when its source conductance is maintained at absolute zero temperature. For a three-frequency mixer (having external terminations at the signal, image, and intermediate frequencies), the single-sideband mixer noise temperature $T_{M_{SSB}}$ is defined in the same way, but with the stipulation that the image conductance of both the noisy and noiseless mixers be maintained at absolute zero temperature.[3]

The effective mean-square input noise current necessary to produce the noise voltage $\langle \delta V_{N_0} \rangle$ at the output, is found using (16):

$$\langle \delta I'^2_{N_1} \rangle = \langle \delta V^2_{N_0} \rangle / |Z'_{01}|^2. \tag{36}$$

This corresponds to input current source $\delta I'_1$ in Fig. 2 and is associated with the impedance $(Z_{e_1} + R_{s_1})$. The corresponding mean-square noise voltage associated with the source impedance Z_{e_1} is $\langle \delta I'^2_{N_1} \rangle |Z_{e_1} + R_{s_1}|^2$. The effective input noise temperature of the mixer T_M is the temperature to which Re $[Z_{e_1}]$ must be heated to generate an equal noise voltage. Hence, using (36),

$$T_M = \frac{\langle \delta V^2_{N_0} \rangle}{4k\Delta f} \frac{|Z_{e_1} + R_{s_1}|^2}{|Z'_{01}|^2 \text{ Re } [Z_{e_1}]}. \tag{37}$$

$\langle \delta V^2_{N_0} \rangle$ is given by (35) in terms of the internal shot and thermal noise sources of the diode and Z'_{01} is an element of the matrix $\boldsymbol{Z}'$ defined in (17).

The single sideband noise figure of the mixer is defined as

$$F_{SSB} = 1 + \frac{T_M}{T_0} \tag{38}$$

where $T_0 = 290$ K by convention.

V. The Microwave Schottky Diode

The Schottky diode is conventionally represented as shown in Fig. 1. The series resistance is assumed equal to its dc value and independent of frequency, while the capacitance exponent γ (5) is assumed independent of voltage. For a diode of the kind used for microwave and millimeter-wave mixers these assumptions are not generally valid, and it is important to include the departures from ideality in the nonlinear and small-signal analyses if accurate results are to be obtained.

A. Series Resistance

There are three effects which cause the series resistance R_s of a diode to differ from the value determined from the dc log I–V curve. These are 1) thermal time-constants in the diode, 2) RF skin effect in the diode material, and 3) the voltage dependence of the depletion-layer width.

It has been shown by Decker and Weinreb [20] that the incremental junction resistance of a diode, measured at a

[3] For the three-frequency mixer a double-sideband noise temperature $T_{M_{DSB}}$ is frequently used. For cases in which the signal and image conversion loss L_{01} and L_{0-1} are equal $T_{M_{DSB}} = \frac{1}{2}T_{M_{SSB}}$. If $L_{01} \neq L_{0-1}$, which is particularly probable when a high IF is used, then $T_{M_{DSB}} = T_{M_{SSB}}/(1 + L_{01}/L_{0-1})$.

low frequency (audio or dc), contains a negative component caused by heating of the diode by the test signal. Thus

$$r_{lf} \triangleq \frac{dv_j}{di_d} = \left.\frac{\partial v_j}{\partial i_d}\right|_T + \left.\frac{\partial v_j}{\partial T}\right|_{i_d} \cdot \frac{dT}{di_d} \tag{39}$$

$$= r_{hf} + \left.\frac{\partial v_j}{\partial T}\right|_{i_d} \cdot \frac{dT}{di_d}. \tag{40}$$

The second term on the RHS of (39) is the (negative) component of the low-frequency junction resistance which results from the diode temperature varying in phase with the test signal. At higher frequencies, above about 10 MHz for our 2.5-μm GaAs diodes, thermal time constants in the diode prevent its temperature from varying appreciably and only the term r_{hf} is measured. It follows that the value of the series resistance R_s deduced from the dc log I–V curve is lower than the true constant temperature value which would be observed at microwave frequencies. For our millimeter-wave diodes the error in R_s is 1–3 Ω [20], [23].

The RF skin effect contributes an additional resistance R_{skin} in series with the diode. R_{skin} is proportional to $\sqrt{f}$ and can be estimated if the diode geometry and resistivity are known [24]. The diode contact wire is also likely to have a significant skin resistance, which should be included in R_{skin}. For our 2.5-μm GaAs diodes R_{skin} is 2–3 Ω at 100 GHz.

The width of the depletion layer in a diode depends on the junction voltage and, therefore, the component of series resistance contributed by the undepleted epitaxial material will also be voltage-dependent. In the present paper we have assumed that this voltage dependence has negligible effect on the performance of the mixer.

B. Junction Capacitance

The simple diode capacitance law, (5), is derived in many texts [21] for planar diodes. If the doping profile at the barrier (or junction) is uniform or linear with distance, the exponent γ has the value $\frac{1}{2}$ or $\frac{1}{3}$, respectively. However, for the very small diameter diodes used at millimeter wavelengths the assumption of a planar device is no longer valid: fringing effects at the edge of the depletion layer are significant and the shape of the depletion layer is voltage-dependent [21]. The simple capacitance law, (5), can still be used provided the exponent γ is allowed to be voltage dependent, i.e., $\gamma \rightarrow \gamma(v_j)$.

VI. Application to Practical Mixers

The mixer analysis presented in the preceeding sections assumes a knowledge of the diode and embedding impedance at all harmonics of the LO and at all the sideband frequencies $\omega_0 + k\omega_p$, $k = 0, \pm 1, \pm 2, \cdots, \pm\infty$. In practice the number of frequencies which can be considered is limited by the ability to make meaningful measurements or calculations of the embedding impedance beyond some frequency limit, and by the size of complex matrix which can be inverted by available computers. The computer time required to solve the nonlinear problem increases rapidly with the number of LO harmonics. It is necessary therefore to work with a finite number N of LO harmonics and a corresponding number $(N + 1)$ of sideband frequencies. The infinite series and matrices of Sections II–IV can then be replaced by finite ones. The electrical implication of such a truncation is that all higher harmonics or sidebands are either open- or short-circuited. In particular, truncation of the Y matrix in (12) implies that all higher sidebands are short-circuited. This is likely to be a good approximation for millimeter-wave mixers because the mean junction capacitance approaches a short circuit for very high frequencies. A similar situation results from ignoring frequencies above $N\omega_p$ in the nonlinear analysis. Using Gwarek's method it is tacitly assumed that the junction voltage v_j has no components above frequency $N\omega_p$. Again this should be a good approximation provided N is high enough.

VII. Conclusion

The nonlinear, small-signal, and noise analysis given in Sections II–V provides the means for accurately determining the performance of microwave and millimeter-wave mixers. In the companion paper, Part 2, the analysis is applied to mixers operating at 87 and 115 GHz. Good agreement with measured results is obtained, and the "anomalous" mixer noise [14] is shown to be primarily shot noise for which the phase relations of down-converted components must be taken into account.

References

[1] H. C. Torrey and C A. Whitmer, *Crystal Rectifiers*, (MIT Radiation Lab. Series, vol. 15). New York: McGraw-Hill, 1948.

[2] W. M. Sharpless, "Wafer-type millimeter-wave rectifiers," *Bell Syst. Tech. J.*, vol. 35, pp. 1385–1402, Nov. 1956.

[3] G. C. Messenger and C. T. McCoy, "Theory and operation of crystal diodes as mixers," *Proc. IRE*, vol. 45, pp. 1269–1283, 1957.

[4] L. Mania and G. B. Stracca, "Effects of the diode junction capacitance on the conversion loss of microwave mixers," *IEEE Trans. Communications*, vol. COM-22, pp. 1428–1435, Sept. 1974.

[5] A. R. Kerr, "Low-noise room-temperature and cryogenic mixers for 80–120 GHz," *IEEE Trans. Microwave Theory Tech.*, vol. MTT-23, pp. 781–787, Oct. 1975.

[6] M. R. Barber, "Noise figure and conversion loss of the Schottky barrier mixer diode," *IEEE Trans. Microwave Theory Tech.*, vol. MTT-15, pp. 629–635, Nov. 1967.

[7] A. A M. Saleh, *Theory of Resistive Mixers*. Cambridge, MA: MIT Press, 1971.

[8] S Egami, "Nonlinear, linear analysis and computer aided design of resistive mixers," *IEEE Trans. Microwave Theory Tech.*, vol. MTT-22, pp. 270–275, Mar. 1974.

[9] M. J. O. Strutt, "Noise figure reduction in mixer stages," *Proc. IRE*, vol 34, no. 12, pp. 942–950, Dec. 1946.

[10] A. van der Ziel and R. L. Waters, "Noise in mixer tubes," *Proc. IRE*, vol. 46, pp. 1426–1427, 1958.

[11] A. van der Ziel, *Noise: Sources, Characterization, and Measurement*. Englewood Cliffs, NJ: Prentice-Hall, 1970

[12] C. S. Kim, "Tunnel diode converter analysis," *IRE Trans. Electron Devices*, vol. ED-8, no. 5, pp. 394–405, Sept 1961.

[13] C. Dragone, "Analysis of thermal shot noise in pumped resistive diodes," *Bell Syst. Tech. J.*, vol. 47, pp. 1883–1902, 1968.

[14] A. R. Kerr, "Anomalous noise in Schottky-diode mixers at millimeter wavelengths," *IEEE MTT-S Int. Microwave Symp., Digest of Technical Papers*, pp. 318–320, May 1975.

[15] D. A. Fleri and L. D Cohen, "Nonlinear analysis of the Schottky-barrier mixer diode," *IEEE Trans. Microwave Theory Tech.*, vol. MTT-21, pp. 39–43, Jan. 1973.

[16] A. R. Kerr, "A technique for determining the local oscillator waveforms in a microwave mixer," *IEEE Trans Microwave Theory Tech.*,

vol. MTT-23, pp. 828–831, Oct. 1975.
[17] W. K. Gwarek, "Nonlinear analysis of microwave mixers," M.S. thesis, MIT, Cambridge, Sept. 1974.
[18] S. O. Rice, "Mathematical analysis of random noise," *Bell Syst. Tech. J.*, vol. 23, no. 3, pp. 282–332, July 1944.
[19] V. R. Bennet, *Electrical Noise*. New York: McGraw-Hill, 1960.
[20] D. R. Decker and S. Weinreb, private communication.
[21] S. M. Sze, *Physics of Semiconductor Devices*. New York: Wiley, 1969 (see p. 90 *et seq.*).
[22] W. Baechtold, "Noise behavior of GaAs field-effect transistors with short gates," *IEEE Trans. Electron Devices*, vol. ED-19, pp. 674–680, 1972.
[23] D. N. Held, "Analysis of room temperature millimeter-wave mixers using GaAs Schottky barrier diodes," Sc.D. dissertation, Department of Electrical Engineering, Columbia University, New York, 1976.
[24] J. A. Calviello, J. L. Wallace, and P. R. Bie, "High performance GaAs quasi-planar varactors for millimeter waves," *IEEE Trans. Electron Devices*, vol. ED-21, pp. 624–630, Oct. 1974.

Conversion Loss and Noise of Microwave and Millimeter-Wave Mixers: Part 2—Experiment

DANIEL N. HELD, MEMBER, IEEE, AND ANTHONY R. KERR, ASSOCIATE MEMBER, IEEE

Abstract—**The theory of noise and conversion loss in millimeter-wave mixers, developed in a companion paper, is applied to an 80–120-GHz mixer. Good agreement is obtained between theoretical and experimental results, and the source of the recently reported "anomalous noise" is explained. Experimental methods are described for measuring the embedding impedance and diode equivalent circuit, needed for the computer analysis.**

I. Introduction

In Part 1 of this paper [1] the theory of microwave and millimeter-wave mixers was presented in a form suitable for analysis by digital computer. The present paper gives the results of such an analysis, comparing computed and measured conversion loss, noise, and output impedance for an 80–120-GHz mixer under various operating conditions.

The significance of this work in relation to earlier work is discussed in the introduction to Part 1, the salient points being that this method of analysis gives unprecedented agreement between theory and experiment and that the "anomalous noise" [2] reported in millimeter-wave mixers is entirely accounted for.

The analysis requires a knowledge of the embedding impedance seen by the diode at a finite number of frequencies, and of the equivalent circuit of the diode, including noise sources. Experimental methods for determining these input quantities are described in Sections II and III. The mixer analysis is described in Section IV and typical sets of theoretical and measured results are shown to be in good agreement. Section V discusses the sources of mixer noise and loss, and small-signal power flow in the mixer.

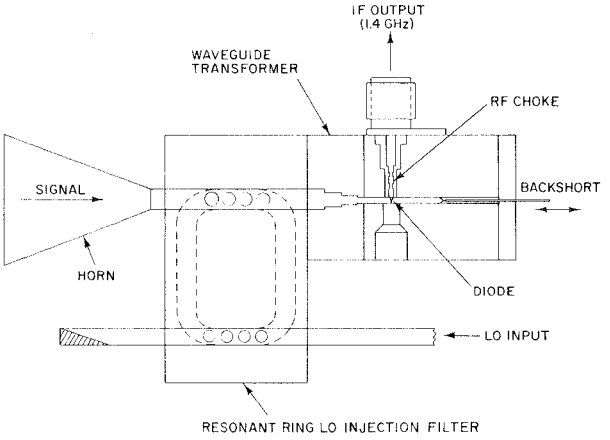

Fig. 1. Cross-section of the 80–120-GHz mixer used in this work.

The mixer used for these experiments is the room-temperature 80–120-GHz mixer described in [3] and is shown here in Fig. 1. It uses a 2.5-μm-diameter GaAs Schottky diode in a quarter-height waveguide mount. The diode was made by Professor R. J. Mattauch at the University of Virginia.

Manuscript received February 18, 1977; revised May 12, 1977.

D. N. Held was with the Department of Electrical Engineering, Columbia University, New York, NY 10027. He is now with the Jet Propulsion Laboratory, California Institute of Technology, Pasadena, CA 91103.

A. R. Kerr is with the NASA Institute for Space Studies, Goddard Space Flight Center, New York, NY 10025.

0018-9480/78/0200-0055$00.75